

Panu Takala
Helena Hänninen
Juha Montonen
Petri Korhonen
Markku Mäkijärvi
Jukka Nenonen
Lasse Oikarinen
Lauri Toivonen
Toivo Katila

Heart rate adjustment of magnetic field map rotation in detection of myocardial ischemia in exercise magnetocardiography

Received: 5 April 2001
Returned for 1. revision: 7 May 2001
1. Revision received: 25 May 2001
Returned for 2. revision: 12 June 2001
2. Revision received: 18 June 2001
Accepted: 20 June 2001

P. Takala, LicSc (✉) · J. Montonen
J. Nenonen · T. Katila
Helsinki University of Technology
Laboratory of Biomedical Engineering
P.O. Box 2200
02015 HUT, Espoo, Finland
Tel.: +358-9/451-5841
Fax: +358-9/451-3182
E-Mail: Panu.Takala@hut.fi

P. Takala · H. Hänninen · J. Montonen
P. Korhonen · M. Mäkijärvi · J. Nenonen
L. Oikarinen · T. Katila
BioMag Laboratory
Helsinki University Central Hospital
00029 HUCH, Helsinki, Finland

H. Hänninen · P. Korhonen · M. Mäkijärvi
L. Oikarinen · L. Toivonen
Division of Cardiology
Helsinki University Central Hospital

Abstract *Aims* We studied the capability of heart rate (HR) adjusted change in multichannel magnetocardiogram (MCG) to detect exercise-induced ischemia. *Methods and results* The MCG and 12-lead ECG were recorded simultaneously during supine exercise testing in 17 healthy controls and 24 patients with single vessel coronary artery disease (CAD). In the MCG analysis, we plotted the orientation of the magnetic field map (MFM) against the HR in each cardiac cycle during recovery. A regression line was fitted to the data and the line slope (degrees/bpm) was determined. In the ECG, the ST-segment depression vs HR (ST/HR) slope was evaluated. The HR adjusted MFM rotation was more extensive in the pooled CAD group, and in all subgroups with different stenosed vessel, than in the control group at the ST-segment ($1.5 \pm 2.1^\circ/\text{bpm}$ vs $0.29 \pm 0.25^\circ/\text{bpm}$, $p < 0.0005$) and at the T-wave apex ($0.95 \pm 0.81^\circ/\text{bpm}$ vs $0.24 \pm 0.25^\circ/\text{bpm}$, $p < 0.0005$). Areas under the receiver operating characteristic curves of the HR adjusted MFM rotation at the ST-segment (88.5%) and the T-wave (86.0%) were higher than the ones without HR adjustment (75.5% and 68.1%, respectively), and higher than the area of ST/HR slope in the ECG (80.2%). *Conclusion* HR adjusted MFM rotation detects transient ischemia independent of the stenosed vessel. HR adjustment improves the performance of the MCG in ischemia detection by the analysis of the ST-segment and the T-wave. The MCG was superior to the 12-lead ECG.

Key words Magnetocardiography – ischemia – coronary artery disease – exercise test – heart rate adjustment

Introduction

Multichannel magnetocardiography (MCG) is a novel, non-invasive and non-contact mapping technique for studying the electromagnetic function of the heart (17). The MCG records the magnetic field induced by the same bioelectric currents that generate the electrocardiogram (ECG). In addition to the morphological features of the MCG, such as the QRS-complex and the ST-segment, the

spatial distribution of the multichannel MCG signal also provides information on the cardiac activity.

The MCG contains information complementary to the ECG (5). It is sensitive to circular currents which can not be detected by the ECG (1) and it is most sensitive to currents tangential to the chest. Since the main direction of normal ventricular activation is radial, from the endocardium to the epicardium, the MCG may display better differentiating power between normal and abnormal myocardial activation than the ECG (16). The MCG has

been used, e.g., in the localization of sources of cardiac arrhythmias (6, 9–11, 21) and in risk stratification after myocardial infarction (4).

Recent studies on exercise MCG have demonstrated its potential to detect transient ischemia. In coronary artery disease (CAD), ischemia induces changes in the magnetocardiographic QT dispersion (2) and in the orientation of magnetic field maps (3, 18). The MCG has also been used to localize transient and chronic ischemia (15). Therefore, the MCG might be a complementary tool to the ECG for the detection of exercise-induced ischemia. Studies on exercise MCG are, however, few and the total number of patients studied is small. Previous studies on exercise MCG have focused on signal averaged data at one or a few intervals of the recovery period, and dynamic changes in ischemia parameters have not been evaluated.

Heart rate adjustment of the ST depression improves the performance of exercise ECG (13). In exercise MCG, the ischemic injury current induces a rotation of magnetic field maps (MFM) (3, 18). We hypothesized that heart rate adjustment of MFM rotation, taking into account the extent of stress, improves the detection of ischemia by the MCG.

Methods

Patients and controls

The study population comprised 41 subjects: 24 middle-aged patients with single vessel CAD, and 17 healthy volunteers (Table 1). At screening, all patients were required to have a significant (> 50 % luminal diameter) stenosis in one of the main coronary branches: left anterior descending (LAD), left circumflex (LCX), or right coronary artery (RCA); 11, 6, and 7 patients, respectively. All

Table 1 Characteristics of the study population

	CAD group				Control group
	Total	LAD	LCX	RCA	Total
Number	24	11	6	7	17
Age (years)	57 ± 9	55 ± 8	59 ± 7	57 ± 12	55 ± 7
Male/Female	14/10	6/5	3/3	5/2	13/4
LVEF (%)	64 ± 8	63 ± 5	70 ± 9	60 ± 7	66 ± 7
Stenosis (%)	86 ± 13	80 ± 15	90 ± 13	92 ± 5	–

Number of subjects or mean ± standard deviation. CAD coronary artery disease patients; LAD patients with left anterior descending coronary artery stenosis; LCX patients with left circumflex coronary artery stenosis; RCA patients with right coronary artery stenosis; LVEF left ventricular ejection fraction

patients had anginal pain and ECG-documented ischemia with ≥ 0.1 mV ST-segment depression in standard upright bicycle exercise testing, normal wall motion and thickness in rest echocardiography, and normal left ventricular systolic function in cine angiography. None of the patients had suffered myocardial infarction or showed abnormal Q-waves or bundle branch block in the 12-lead ECG. All patients were clinically stable and under appropriate medication during the study: 21 patients were on β-blockers, 5 patients on calcium antagonists, and 19 patients on long-acting nitrates. There was no significant difference in age, weight, height or body surface area between the patients and controls. The controls did not have history of hypertension, smoking, or heart disease in the family, and they had normal findings in the echocardiography at rest and in the exercise ECG. All subjects gave their informed consent for the study. The study was performed according to the Declaration of Helsinki and the local ethics committee approved it.

Exercise magnetocardiography

All subjects underwent supine exercise MCG recordings in a magnetically shielded room (14). The MCG signals were recorded over the chest with a 67 channel cardiomagnometer covering a circular area with a diameter of 30 cm over the chest (8). The center of the sensor array was placed 15 cm below the jugular notch and 5 cm to the left of the midsternal line without skin contact (Fig. 1).

Stress was provoked using a laboratory-made non-magnetic ergometer designed for cardiomagnetic measurements. A baseline recording of five minutes at rest preceded a graded exercise test with two minute load steps. The recording was sustained up to ten minutes postexercise. The cessation criteria were severe fatigue or dyspnea, severe chest pain, progressive decrease or abnormal elevation of systolic blood pressure, or repetitive ventricular arrhythmias. Blood pressure was measured at each load level. The 12-lead ECG was recorded simultaneously with the MCG. Both the MCG and the ECG signals were band-pass filtered to 0.03 – 300 Hz and digitized with a sampling rate of 1000 Hz.

Data analysis

An automated analysis method was used to extract the magnetic field maps (MFM) of the ST-segment and the T-wave from each cardiac cycle recorded during the ten minute recovery period (18). Exercise data were not analyzed due to magnetic noise in some of the first measurements. A time point of steepest slope was first determined within the QRS complex in one cardiac cycle. Offsets from this point to the beginning and the end of the QRS complex, as well as to the signal baseline at the PQ

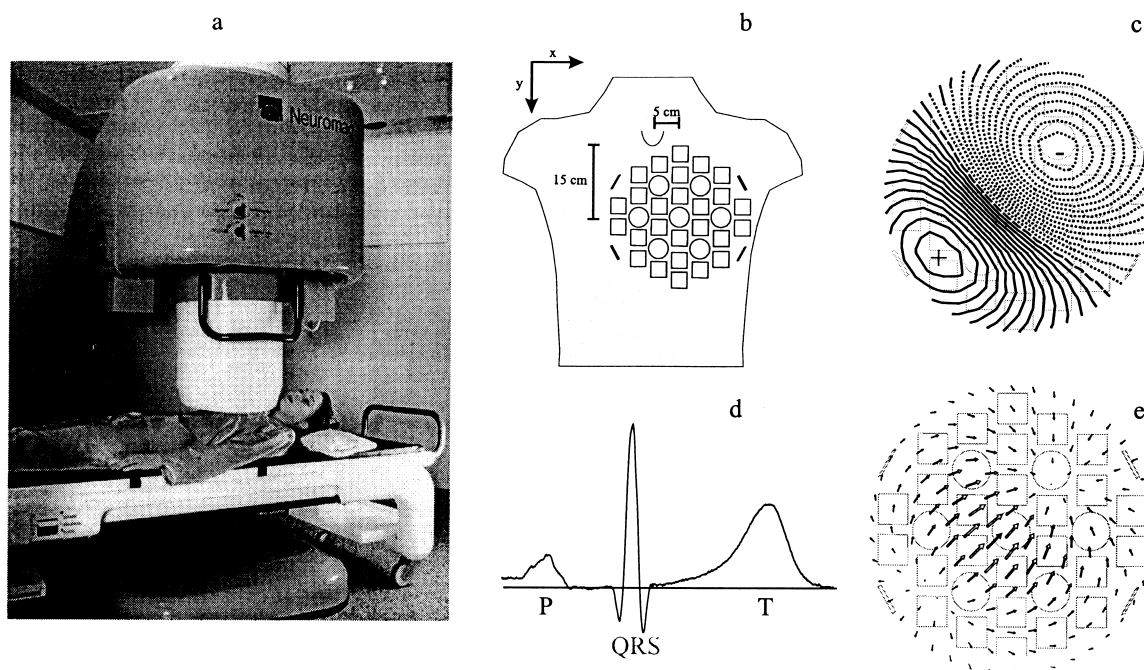


Fig. 1a The 67 channel cardiomagnetometer. **b** The positioning of the sensor array over the chest. The gradiometer sensors record the spatial change of the magnetic field component B_z normal to the sensor plane. Planar sensor units recording $\partial B_z / \partial x$ and $\partial B_z / \partial y$ are marked with squares and co-axial gradiometers recording $\partial B_z / \partial z$ are indicated by circles. **c** A magnetic field map (MFM) illustrating the distribution of B_z over the chest at one time point. Positive magnetic flux, indicated by solid lines, is directed towards the chest. **d** An example of the MCG signal on one channel. **e** Orientation and strength of the spatial change of the magnetic field on the measurement plane, the surface gradient, calculated from the MFM in **c**.

interval, were found manually. The corresponding time points in signal morphology were then automatically found in all beats. The T-wave apex time points were also determined automatically in all cardiac cycles (18). The ST-segment was defined as the second quarter of the time interval from the QRS complex offset to the T-wave apex (Fig. 2). A non-linear baseline estimate was calculated and subtracted from the signal on all channels (7). MFMs of the ST-segment and the T-wave were obtained by calculating the mean value of the MCG signal over the ST-segment, and over 20 ms of data at the T-wave apex in all cardiac cycles. In the ECG, the signal mean over the ST-segment on each lead was extracted for further analysis.

To improve signal to noise ratio, the sequence of MFMs extracted from the recovery data was mean filtered by replacing each map by the mean of the map itself and five maps preceding and following it (18). A surface gradient method was used for calculating the orientations of the filtered MFMs (3, 18). Briefly, the orientation of the largest spatial change in the field distribution was found first (Fig. 1e). The angle between that direction and

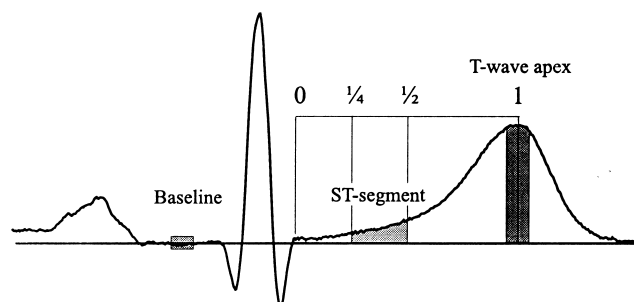


Fig. 2 Magnetic field maps were formed using the mean of the signal over the ST-segment and 20 ms interval on the T-wave apex on all channels. The signal baseline was the average value of the signal over 20 ms on the PQ interval. ST-segment was defined as the second quarter of the time interval from the QRS offset to T-wave apex.

the patient's right-left line was then defined as the MFM orientation (3).

Quantification of change in the magnetic field maps

The orientations of the MFMs at the ST-segment during the recovery period, and the orientations at the T-wave from one to ten minutes postexercise were the source data for quantifying the change in the MCG during the recovery. The mean and standard deviation (SD) of the

angle values over the ten minute recovery period were first calculated in each subject. To reject artifacts, angle values deviating more than $2 \times SD$ from the mean were discarded from further analysis. Thereafter, the MFM angle of each cardiac cycle was plotted against the corresponding instantaneous heart rate, measured from the R-R interval, and a regression line was fitted to the data. The absolute value of the line slope was calculated both for the ST-segment data (MFM ST/HR slope) and the T-wave data (MFM T/HR slope) of each subject.

Heart rate adjustment of ST-segment depression in the ECG

For each ECG lead, excluding aVL, aVR, and V₁, the ST-segment amplitudes of all cardiac cycles during the recovery were plotted against the heart rate. The values outside the interval determined by the average ST-level $\pm 2 \times SD$ were considered as noise and discarded from the analysis. A regression line was fitted to the data, and the steepest negative line slope within all leads was calculated (ECG ST/HR slope). In addition, the ST-segment level was measured from signal averaged data immediately after exercise (3).

Quantification of the signal averaged MCG

Orientations of the MFMs at the ST-segment and the T-wave were measured from selectively averaged data at rest, immediately after exercise, and four minutes post-exercise (3). The orientations were defined in a similar manner as in the analysis of non-averaged data, described above.

Table 2 ST-segment and T-wave MFM angle/HR slopes ($^{\circ}$ /bpm), and ST/HR slope in ECG (μ V/bpm)

Group	MFM ST/HR	MFM T/HR	ECG ST/HR
Controls	0.29 ± 0.25	0.24 ± 0.25	-1.0 ± 0.60
CAD	1.5 ± 2.1^1	0.95 ± 0.81^1	-2.4 ± 1.7^2
LAD	2.2 ± 3.0^2	0.68 ± 0.54^2	$-2.4 \pm 2.0^{3,4}$
LCX	0.97 ± 0.63^2	1.1 ± 0.78^2	-2.9 ± 1.8^2
RCA	0.91 ± 0.62^2	1.2 ± 1.1^3	-2.0 ± 1.2^4

Mean \pm standard deviation. ¹ $p < 0.0005$; ² $p > 0.005$; ³ $p > 0.01$; ⁴ $p < 0.05$ comparing patients and controls. MFM magnetic field map; HR heart rate; bpm beats per minute; CAD coronary artery disease patients; LAD patients with left anterior descending coronary artery stenosis; LCX patients with left circumflex coronary artery stenosis; RCA patients with right coronary artery stenosis

Statistical analysis

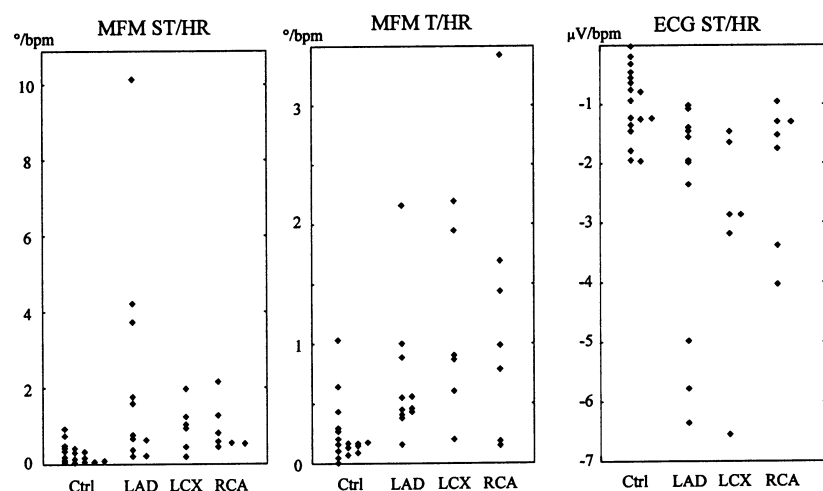
The Mann-Whitney U test was used for evaluating the differences between CAD patients and controls. Value $p < 0.05$ was considered statistically significant.

Results

Heart rate adjusted MCG

The HR adjusted MFM rotation was more extensive in the CAD patient group than in the control group during the recovery period of exercise testing. At the ST-segment, the regression lines of the MFM rotation had higher slope values in the pooled CAD patient group, as

Fig. 3 ST-segment (left) and T wave (center) magnetic field map (MFM) angle/heart rate (HR) slopes and the ST/HR slope in the ECG (right) of all subjects. Ctrl controls, LAD patients with left anterior descending coronary artery stenosis, LCX patients with left circumflex coronary artery stenosis, RCA patients with right coronary artery stenosis. For numerical data, see Table 2.



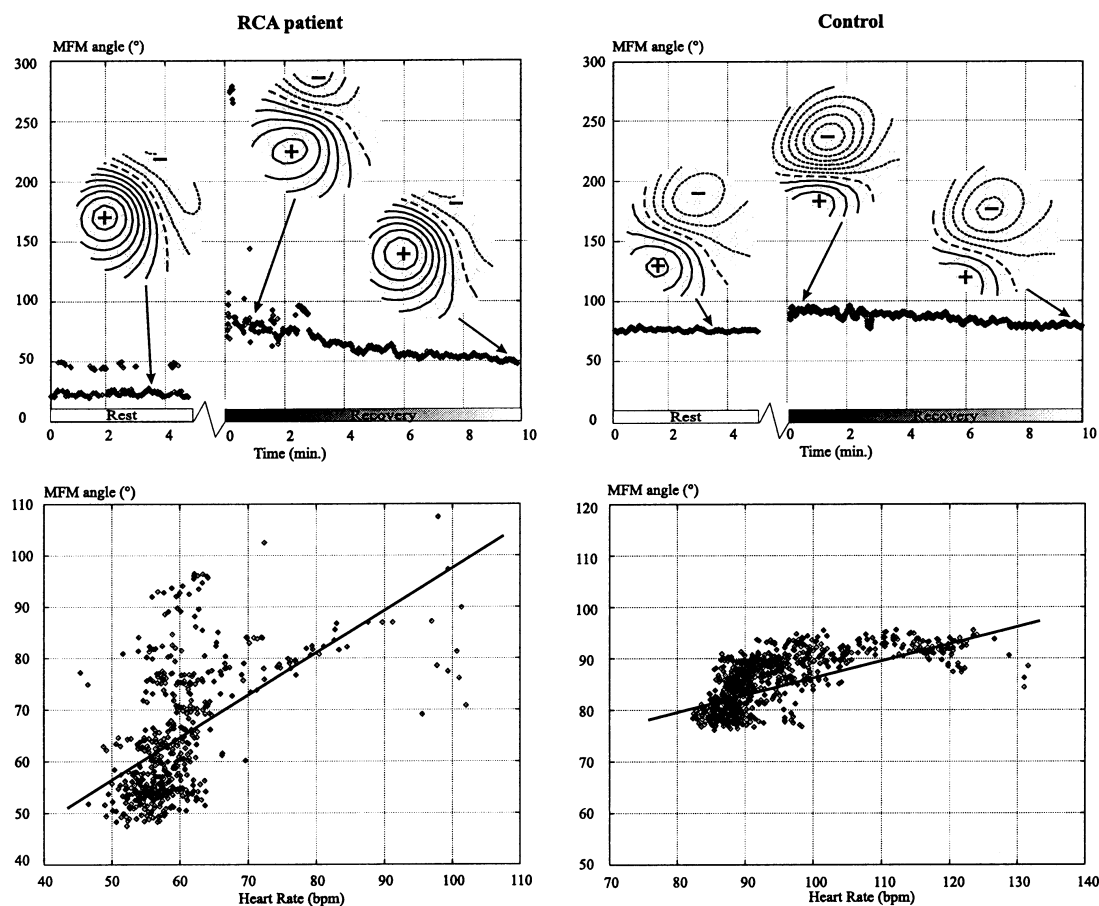


Fig. 4 ST-segment magnetic field map (MFM) angle of each cardiac cycle recorded in one RCA patient (left) and in one healthy control (right), and examples of field distributions. In the upper panels, the MFM angles at rest and during the recovery from exercise are plotted against time. Data during exercise have been omitted. After exercise the angle is tilted compared to rest, and during the recovery it returns close to the baseline value. In the RCA patient, the rotation due to exercise is more extensive than in the control. Arrows indicate the time points and angle values for the MFMs shown. The step between two isofield lines in the maps is 0.5 pT. In the lower panels, the MFM data is plotted against the heart rate. Lines through the data indicate the regression lines used for the quantification of the change in the MFM angles. For the patient the line slope is 0.81°/bpm and for the control it is 0.34°/bpm.

well as in all patient subgroups, than in the control group (Table 2, Fig. 3, Fig. 4). At the T-wave the regression line slopes were also steeper in the CAD patient group and in all patient subgroups than in the control group (Table 2, Fig. 3, Fig. 5).

In some CAD patients the MFMs had a monopolar pattern without a clear maximum of the spatial MCG signal gradient during recovery. Because the maximum gradient was used to determine the MFM orientation, sudden changes in its location resulted in an abrupt

change in the MFM angle and gave rise to especially high regression line slope values in such patients. This resulted in a high standard deviation in these patients' MFM angle parameters (Table 2, Fig. 3). In the control group the average slope values and their standard deviations were small.

Signal averaged MCG

In the signal averaged MCG, the MFM angles at the ST-segment were higher in the CAD patient group than in the control group at cessation of exercise (CAD, $162 \pm 69^\circ$; controls, $106 \pm 49^\circ$, $p < 0.01$) and four minutes post-exercise (CAD, $157 \pm 45^\circ$; controls, $111 \pm 50^\circ$; $p < 0.01$), but not at rest. At the T-wave apex, the angles in the CAD group did not differ significantly compared to the control group at rest, immediately after exercise ($p = \text{N.S.}$, both), or four minutes postexercise ($p = 0.05$). The T-wave performed better in ischemia detection 4 minutes postexercise than immediately after exercise.

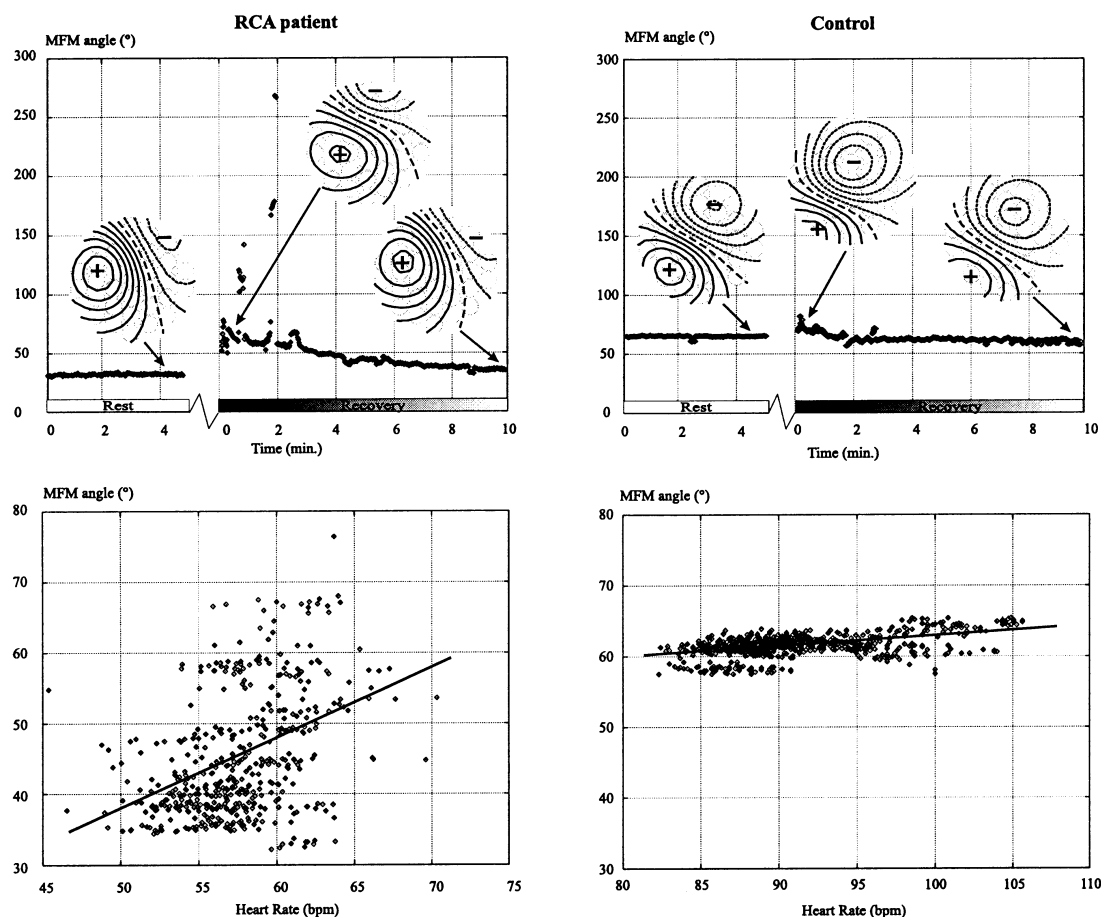


Fig. 5 T-wave magnetic field map (MFM) angle of each cardiac cycle recorded in the same subjects as in Fig. 4. Left, an RCA patient; right, a healthy control. The format of the presentation is the same as in Fig. 4. At rest the MFM angle has an approximately constant value. After exercise the MFM angle is tilted more in the RCA patient than in the control, and in the control the angle returns faster to the baseline value. The step between two isofield lines in the MFMs shown is 2 pT. In the lower panels, data from one to ten minutes postexercise are plotted against the heart rate. For the RCA patient the regression line slope is 0.99°/bpm and for the control it is 0.15°/bpm.

■ 12-lead ECG

In the 12-lead ECG the ST-segment depression/HR slope during the recovery was steeper in the CAD patient group and in all patient subgroups compared to the control group (Table 2). Of the 24 patients, 11 had an ST-segment depression ≥ 0.1 mV immediately after exercise. The

maximum ST depressions were 0.09 ± 0.08 mV in the CAD group and 0.02 ± 0.02 mV in the control group. The maximum rate pressure products in supine stress testing for the MCG were lower than in upright bicycle stress testing (all subjects; mean 21 ± 6 and 27 ± 5 mmHg \times bpm $\times 10^{-3}$, respectively, $p < 0.001$).

■ Receiver operating characteristic curves

The heart rate adjusted MFM rotation at the ST-segment had a higher sensitivity to CAD than the MFM orientation at the ST-segment immediately after exercise at almost all values of specificity (Fig. 6). It also had a higher or equal sensitivity compared to the heart rate adjusted ST-segment depression in the ECG at all values of specificity. At the T-wave, the heart rate adjusted MFM rotation had an equal or higher sensitivity compared to the MFM orientation at the T-wave 4 minutes postexercise, independent of the required specificity.

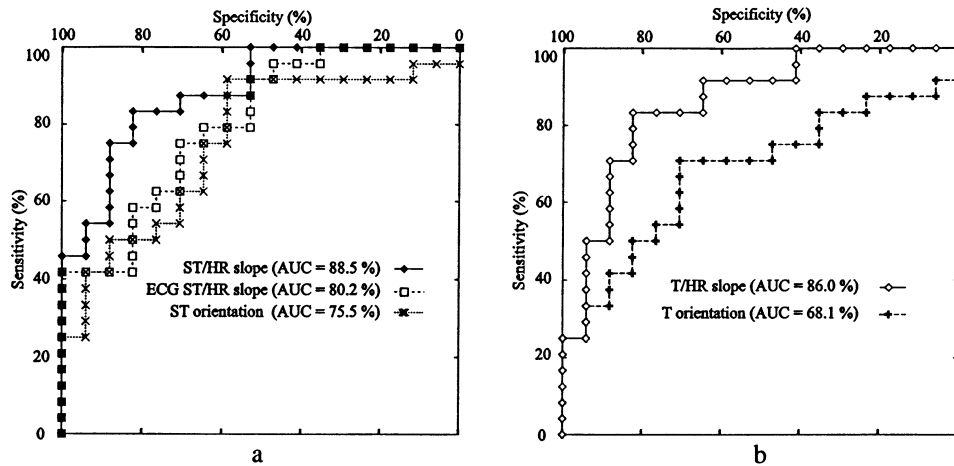


Fig. 6a Receiver operator characteristic (ROC) curves for heart rate adjusted magnetic field map (MFM) rotation (ST/HR slope), heart rate adjusted ST-segment depression in ECG (ECG ST/HR slope), and MFM orientation at the ST-segment in signal averaged data immediately after exercise (ST orientation). Areas under ROC curve (AUC) are indicated as percentages. **b** ROC curves and AUCs for heart rate adjusted MFM rotation at the T-wave (T/HR slope) and MFM orientation at the T-wave 4 minutes postexercise (T orientation).

Discussion

Our results show that heart rate adjustment improves detection of exercise-induced ischemia by the MCG. Heart rate adjusted magnetic field map rotation detects ischemia caused by a stenosis in any of the major coronary artery branches. The rotation of the MFM at the ST-segment and the T-wave, adjusted to heart rate, was more extensive in all stenosed vessel subgroups as well as in the pooled CAD patient group when compared to the control group. Importantly, the heart rate adjustment also improved ischemia detection by the T-wave data.

In the beat-to-beat analysis of the T-wave in the present work, we found a small fast-decaying change in the MFM orientation immediately after exercise in several controls (Fig. 5). This change might explain the better diagnostic power of the T-wave in the MCG at few minutes into recovery compared to immediately postexercise, reported by Hänninen et al. (3). They evaluated the MFM orientation at the ST-segment and the T-wave in signal averaged data of single vessel CAD patients and controls immediately after exercise and 4 minutes postexercise. At the T-wave apex, a difference between patients and controls was found only at 4 minutes postexercise. Changes in the MCG of healthy subjects were found also by Brockmeier et al. after pharmacological stress (1).

In the present study, the dynamic change in the MFM orientation during exercise testing was found to contain

information on ischemia. Van Leeuwen et al. determined the MFM orientation over the QRST interval at rest in healthy controls, patients with myocardial infarction (MI), and CAD patients without MI (19). Both patient groups showed deviations of the MFM angles compared to controls, especially at the T-wave apex and T-wave offset. The ischemia-induced changes in the MFM orientation at the T-wave could affect the QT interval duration and its spatial distribution. Hailer et al. studied CAD patients and controls using multichannel MCG during pharmacologically induced stress (2). They found a significant difference between the two groups in the spatial distribution of QT intervals in the MCG both at rest and during stress.

Of 24 patients, 11 had an ST-segment depression ≥ 0.1 mV immediately after exercise in the ECG, recorded simultaneously with the MCG. The maximum rate pressure products during the MCG were also lower than in the upright exercise testing. This suggests that the ischemia, induced in the supine exercise MCG recording, was not as severe as in the upright exercise testing where all patients fulfilled the inclusion criterion of ST-segment depression ≥ 0.1 mV. In spite of this, all patient subgroups had a steeper MFM ST/HR slope than the control group, independent of the diseased vessel. Interestingly, the MFM T/HR slope was also steeper in all patient subgroups than in the control group. The areas under the receiver operating characteristic curves of the heart rate adjusted MFM parameters were larger than that of the heart rate adjusted ST-segment depression in the ECG. Therefore, the MCG might be more sensitive than the ECG to ischemia at the recovery period of exercise testing. Compared to 12-lead ECG, multichannel MCG has more channels and better spatial coverage. Thereby, the amount of information is higher in the MCG than in the ECG.

Two methods of heart rate adjustment of ST-segment depression have evolved in the 12-lead ECG (13). The

simpler ST-segment/HR index is derived by dividing the maximal change in ST-segment depression during exercise by the total change in heart rate from rest to peak exercise. In the other method, ST-segment/HR slope calculation, linear regression analysis is performed from the end of exercise to earlier intermediate stage data in each lead. The highest ST-segment/HR slope with a statistically significant correlation coefficient among all leads, including CM₅ but excluding aVR, aVL, and V₁, is taken as the test finding. Both in the ST-segment/HR index and in the ST-segment/HR slope calculation, the source data is obtained at the end of each stage of exercise (13). Our study focused on the data recorded during the recovery, and the exercise data were excluded from the analysis. Contrary to signal averaging, each cardiac cycle yielded one data point for the regression analysis. The heart rate adjustment method applied to the MFM rotation and to the ST-segment level in the ECG in this work resembles the previously reported ST-segment/HR slope calculation as it incorporates in the regression analysis all data points during the recovery. It does not, however, focus on the most rapid change in the MFM orientation and in that respect it is similar to the ST-segment/HR index.

The inter-individual variation in the dependence between MFM orientation and HR was extensive during the 10 minutes of recovery. Monopolar maps in some patients resulted in abrupt changes in the MFM orientation, defined by the maximum gradient. In general, the dependence between MFM orientation and heart rate was not linear in the patients. We used linear regression merely to quantify the change of the MFM orientation and to adjust it with the corresponding change of HR. Although the linear model is not wholly appropriate, it is the simplest way to reflect the differences in orientation observed in the data evaluated in this work.

The measurements reported in this paper are among the first multichannel exercise MCG mappings and magnetic noise corrupted some of the data during exercise. Therefore, only the recovery data were used for the analysis. Lower noise will allow using the exercise data and the comparison between the MCG and ECG during exercise. Analysis of MCG data both during exercise and recovery would also allow the study of rate recovery loop in the MCG (12). To attain a lower noise level, pharmacological stress can also be used in MCG measurements (2, 20).

The ischemic injury current in the heart, caused by subendocardial ischemia, is directed from the lower left to the upper right thorax. In theory, such a current induces a magnetic flux toward the chest in the upper left thorax and outward from the chest at the lower central thorax. When such ischemic signal distribution is superimposed over a normal MFM, it might cause the rotation

in the MFMs (18). The direction of the MFM rotation due to ischemia would then depend on the orientation of the normal MFM as well as on the orientation of the ischemia-induced contribution in the MFM which is dependent on the direction of the ischemic injury current. We evaluated only the extent, not the direction, of the heart rate adjusted MFM rotation and used the absolute value of the line slope as a parameter to detect ischemia. Further work is needed to study whether the direction of the rotation can be utilized to identify the culprit vessel.

Limitations of the study

The results should be considered as preliminary, due to the small number of patients. Only the postexercise data were analyzed, due to magnetic noise during exercise in some of the very first recordings. With further experience in MCG stress testing, exercise data suitable for analysis can also be recorded. This will provide better comparison with the standard ECG ST/HR slope and index methods. In spite of non-linear dependence between MFM orientation and HR, linear regression was used for quantifying the change of the MFM orientation and adjusting it with the corresponding change of HR. We did not assess ischemia detection in the presence of myocardial infarction or multivessel disease. Most of the CAD patients were on β -blockers at the time of the study, resulting in lower heart rates and less ST-depression in stress testing. This may have hampered the ischemia detection in the MCG. Also, the effect of β -blockers on the MCG is not known. Further studies with more patients are needed to determine the sensitivity and specificity of the method.

Conclusion

Heart rate adjustment improves the performance of the exercise MCG in ischemia detection. Exercise-induced ischemia caused by a stenosis in any of the major coronary artery branches can be detected by heart rate adjusted change in magnetic field map orientation. The heart rate adjustment also improves the detection of ischemia by the T-wave. The MCG performed better than the 12-lead ECG when data recorded postexercise was analyzed.

Acknowledgments This work was supported by the Jenny and Antti Wihuri Foundation, the Foundation of Technology in Finland, and the Academy of Finland.

References

1. Brockmeier K, Schmitz L, Chavez J, Burghoff M, Koch H, Zimmerman R, Trahms L (1997) Magnetocardiography and 32-lead potential mapping: repolarization in normal subjects during pharmacologically induced stress. *J Cardiovasc Electrophysiol* 8: 615–626
2. Hailer B, Van Leeuwen P, Lange S, Wehr M (1999) Spatial distribution of QT dispersion measured by magnetocardiography under stress in coronary artery disease. *J Electrocardiol* 32: 207–216
3. Hänninen H, Takala P, Mäkijärvi M, Montonen J, Korhonen P, Oikarinen L, Nenonen J, Katila T, Toivonen L (2000) Detection of exercise-induced myocardial ischemia by multichannel magnetocardiography in single vessel coronary artery disease. *Annals of Noninvasive Electrocardiology* 5: 147–157
4. Korhonen P, Montonen J, Mäkijärvi M, Katila T, Nieminen MS, Toivonen L (2000) Late fields of the magnetocardiographic QRS complex as indicators of propensity to sustained ventricular tachycardia after myocardial infarction. *J Cardiovasc Electrophysiol* 11: 413–420
5. Lant J, Stroink G, ten Voorde B, Horacek BM, Montague TJ (1990) Complementary nature of electrocardiographic and magnetocardiographic data in patients with ischemic heart disease. *J Electrocardiol* 23: 315–322
6. Leder U, Hauelsen J, Huck M, Nowak H (1998) Non-invasive imaging of arrhythmogenic left ventricular myocardium after infarction. *Lancet* 352: 1825
7. Meyer C, Kaiser H (1977) Electrocardiogram baseline noise estimation and removal using cubic splines and state-space computation techniques. *Comput Biomed Res* 10: 459–470
8. Montonen J, Ahonen A, Hämäläinen M, Ilmoniemi RJ, Laine P, Nenonen J, Paavola M, Simelius K, Simola J, Katila T (2000) Magnetocardiographic functional imaging studies in the BioMag laboratory. In: Aine C, Okada Y, Stroink G, Swithenby S, Wood C (eds) *Biomag 96, Proceedings of the Tenth International Conference on Biomagnetism*. Springer-Verlag, New York, pp 494–497
9. Moshage W, Achenbach S, Göhl K, Bachmann K (1996) Evaluation of the noninvasive localization accuracy of the cardiac arrhythmias attainable by multichannel magnetocardiography (MCG). *Int J Cardiac Imaging* 12: 47–59
10. Nenonen J, Mäkijärvi M, Toivonen L, Forsman K, Leiniö M, Montonen J, Järvinen A, Keto P, Hekali P, Katila T, Siltanen P (1993) Noninvasive magnetocardiographic localization of ventricular preexcitation in Wolff-Parkinson-White syndrome using a realistic torso model. *Eur Heart J* 14: 168–174
11. Oeff M, Burghoff M (1994) Magnetocardiographic localization of the origin of ventricular ectopic beats. *Pacing Clin Electrophysiol* 17: 517–522
12. Okin P, Ameisen O, Kligfield P (1989) Recovery phase pattern of ST segment depression in the heart rate domain: identification of coronary artery disease by the rate recovery loop. *Circulation* 80: 533–541
13. Okin P, Kligfield P (1995) Heart rate adjustment of ST segment depression and performance of the exercise electrocardiogram: a critical evaluation. *J Am Coll Cardiol* 25: 1726–1735
14. Paavola M, Ilmoniemi R, Sohlström L, Meinander T, Penttinen A, Katila T (2000) High performance magnetically shielded room for clinical measurements. In: Aine C, Okada Y, Stroink G, Swithenby S, Wood C (eds) *Biomag 96, Proceedings of the Tenth International Conference on Biomagnetism*. Springer-Verlag, New York, pp 87–90
15. Pesola K, Hänninen H, Lauerma K, Lötjönen J, Mäkijärvi M, Nenonen J, Takala P, Voipio-Pulkki L-M, Toivonen L, Katila T (1999) Current density estimation on the left ventricular epicardium. A potential method for ischemia localization. *Biomed Tech (Berl)* 44S2: 143–146
16. Siltanen P (1989) Magnetocardiography. In: MacFarlane P, Lawrie T (eds) *Comprehensive Electrocardiology 2*. Pergamon Press, New York, pp 1405–1438
17. Stroink G, Moshage W, Achenbach S (1998) Cardiomagnetism. In: Andrä W, Nowak H (eds) *Magnetism in Medicine*. Wiley VCH, Berlin, pp 136–189
18. Takala P, Hänninen H, Montonen J, Mäkijärvi M, Nenonen J, Toivonen L, Katila T (2001) Beat-to-beat analysis method for magnetocardiographic recordings during interventions. *Phys Med Biol* 46: 975–982
19. Van Leeuwen P, Hailer B, Lange S, Donker D, Grönemeyer D (1999) Spatial and temporal changes during the QT-interval in the magnetic field of patients with coronary artery disease. *Biomed Tech (Berl)* 44S2: 139–142
20. Van Leeuwen P, Hailer B, Klein A, Lukat M, Enke M, Lux R, Grönemeyer D (2001) Electric and magnetic QT iso-integral maps in patients with and without coronary artery disease under pharmacologically induced stress. In: Nenonen J, Ilmoniemi RJ, Katila T (eds) *Biomag2000, Proceedings of the 12th International Conference on Biomagnetism*. Espoo, Helsinki University of Technology, pp 557–560
21. Weismüller P, Abraham-Fuchs K, Killman R, Richter P, Harer W, Höher M, Kochs M, Eggeling T, Hombach V (1993) Magnetocardiography: three-dimensional localization of the origin of ventricular late fields in the signal-averaged magnetocardiogram in patients with ventricular late potentials. *Eur Heart J* 14: E61–E68